Dynamical relaxation of correlators in periodically driven integrable quantum systems

Sreemayee Aditya,[1] Sutapa Samanta,[2] Arnab Sen,[2] K. Sengupta,[2] and Diptiman Sen[1]
[1]*Centre for High Energy Physics, Indian Institute of Science, Bengaluru 560012, India*
[2]*School of Physical Sciences, Indian Association for the Cultivation of Science, Jadavpur, Kolkata 700032, India*

(Received 14 December 2021; revised 14 February 2022; accepted 23 February 2022; published 3 March 2022)

We show that the correlation functions of a class of periodically driven integrable closed quantum systems approach their steady-state value as $n^{-(\alpha+1)/\beta}$, where n is the number of drive cycles and α and β denote positive integers. We find that, generically, $\beta = 2$ within a dynamical phase characterized by a fixed α; however, its value can change to $\beta = 3$ or $\beta = 4$ either at critical drive frequencies separating two dynamical phases or at special points within a phase. We show that such decays are realized in both driven Su-Schrieffer-Heeger (SSH) and one-dimensional (1D) transverse field Ising models, discuss the role of symmetries of the Floquet spectrum in determining β, and chart out the values of α and β realized in these models. We analyze the SSH model for a continuous drive protocol using a Floquet perturbation theory which provides analytical insight into the behavior of the correlation functions in terms of its Floquet Hamiltonian. This is supplemented by an exact numerical study of a similar behavior for the 1D Ising model driven by a square pulse protocol. For both models, we find a crossover timescale n_c which diverges at the transition. We also unravel a long-time oscillatory behavior of the correlators when the critical drive frequency, ω_c, is approached from below ($\omega < \omega_c$). We tie such behavior to the presence of multiple stationary points in the Floquet spectrum of these models and provide an analytic expression for the time period of these oscillations.

DOI: 10.1103/PhysRevB.105.104303

I. INTRODUCTION

Nonequilibrium dynamics of closed quantum systems has been the subject of intense research activity in the recent past [1–7]. Theoretical studies on the subject focused initially on quench [8–10] and ramp [11–16] protocols. However, recently, the focus in the field has shifted to periodically driven systems [5–7]. More recently, quasiperiodic and aperiodically driven systems have also been studied [17–21]. The experimental signatures of such dynamics have been investigated in the context of ultracold atoms in optical lattices [22–27].

Quantum systems driven out of equilibrium via a periodic protocol host several phenomena which are not seen in those driven by a quench or a ramp. These include the generation of drive-induced topological states of matter [28–30], realization of Floquet time crystals [31–33], and phenomena such as dynamical localization [34–37], dynamical freezing [38–40], and drive-induced tuning of ergodicity[41,42]. These properties of periodically driven systems, having a time period T, are most easily understood from their Floquet Hamiltonian H_F which is related to their unitary evolution operator U via the relation $U(T, 0) = \exp[-iH_F T/\hbar]$ [7].

The presence of dynamical transitions constitutes yet another interesting phenomenon in periodically driven closed quantum systems [43–49]. Such transitions can be categorized into two distinct classes. The first involves nonanalyticities of the return probability of its wave function; these nonanalyticities show up as cusps in Loschmidt echoes [43]. Such transitions can be related to Fischer zeros of the complex partition function of the driven system [43,44]. In contrast, the second class of transitions constitutes a change in the long-time behavior of the correlation functions of a periodically driven integrable quantum system as a function of the drive frequency [46,47]. Such a transition results from a change in the extrema of the eigenvalues of the Floquet Hamiltonian H_F as a function of the drive parameters; the signature of such transitions can be deciphered from the study of local correlation functions of such models [46,47]. The study of such transitions has also been extended to integrable models with long-ranged interactions [47] and those coupled to an external bath [48]. The characteristics of the correlation function in the two dynamical phases across the transition have been studied in detail. It was shown that for a d-dimensional integrable system after n drive cycles and for large n, these correlators decay as $n^{-(d+2)/2}$ in the high-frequency regime and as $n^{-d/2}$ in the low-frequency regime. However, the behavior of the system at a dynamical critical point and its vicinity has not been studied previously.

In this paper, we study the properties of correlation functions for general driven 1D integrable quantum systems which have a simple representation in terms of free fermions. Our analysis holds for several 1D spin systems such as the Ising model in a transverse field, the XY model, and the 1D Kitaev chain. All these models allow for a simple fermionic representation via a Jordan-Wigner transformation leading to a quadratic, exactly solvable Hamiltonian [50]. In addition, it is also applicable to charge- or spin-density-wave systems described by the SSH model [51].

The central points that emerge from such a study are as follows. First, we show that all local fermionic correlation

functions of such driven models decay to their steady-state value according to the relation

$$C_x(nT) \sim n^{-(\alpha+1)/\beta}, \tag{1}$$

where α and β are positive integers and x indicates the spatial coordinate. We note that only the case of $\beta = 2$ and $\alpha = 0, 2$ has been discussed in earlier studies [46–48]; these are reproduced as special cases of the general result given by Eq. (1). We show that such a result is tied to the stationary point structure and symmetry properties of the Floquet spectrum of the system. We identify the condition for the existence of anomalous powers ($\beta \neq 2$) for the driven system and estimate a crossover scale, n_c, after which the system is expected to deviate from the anomalous ($\beta \neq 2$) scaling toward the generic ($\beta = 2$) one. This crossover scale diverges at specific points in the parameter space of the driven system; we chart out the condition for the realization of such points in terms of its Floquet spectrum. Second, we provide a specific example of such decay with $\beta \neq 2$ in the context of simple models. To this end, we study the driven SSH model using a continuous drive protocol. We find the realization of decay exponents $-1/3$ corresponding to $\beta = 3$ and $\alpha = 0$. We analytically calculate the corresponding Floquet Hamiltonian within a Floquet perturbation theory (FPT) [7,52,53] which provides insight into the structure of the Floquet spectrum and the correlation functions of the model. Such analytical results are shown to match closely with exact numerical studies. Third, we identify a long-time coherent oscillation of the correlation function of such models when the drive frequency is near to but less than a critical drive frequency. We show that the oscillation is a consequence of the presence of multiple stationary points in the Floquet spectrum of the SSH model; consequently, it is absent at drive frequencies higher than the critical frequencies. We provide an analytic expression for the time period of the oscillation which matches our numerical results. Fourth, we analyze the Ising model driven by a square pulse protocol and show the existence of anomalous decay exponents corresponding to $\beta = 4$ at the first dynamical transition. We provide a detailed analysis of the crossover scale around this transition. Furthermore, we note that at the reentrant transitions present in this model, the correlation functions show a decay characterized by an exponent of $-1/3$, which is similar to that in the SSH model. In addition, near the first transition, we unravel the long-time oscillatory nature of the correlation functions when the critical drive frequency is approached from below (lower frequency); this feature is absent when the transition is approached from above. We provide an explanation of such behavior using the properties of the Floquet spectrum of the driven models. Finally, our analysis identifies a crossover scale n_c which diverges at the dynamical transition characterized by the critical drive frequency ω_c: $n_c \sim |\omega - \omega_c|^{-\beta_0/(\beta_0 - a_0)}$, where $a_0 = 1$ or 2 depending on the symmetry of the model, and $\beta_0 > a_0$ corresponds to the order of the second term in expansion of the Floquet energy around the transition point. For $n > n_c$, the decay of the correlation function follows a generic exponent corresponding to $\beta = 2$; below n_c, the decay is characterized by $\beta > 2$. We validate such a power-law divergence of n_c from exact numerics for both the Ising and the SSH model.

The rest of the paper is as follows. In Sec. II, we analyze the correlation functions of a driven fermion model and provide a detailed derivation of Eq. (1). This is followed, in Sec. III, by a study of the driven SSH model which provides concrete examples of the scaling laws discussed. Next, in Sec. IV, we study the scaling behavior of the correlation functions of the periodically driven 1D Ising model in a transverse field. Finally, we summarize our results and conclude in Sec. V.

II. GENERAL RESULTS

In this section, we shall discuss the general behavior of correlation functions of periodically driven 1D integrable models. In what follows, we shall consider a 1D integrable model whose Hamiltonian is given by

$$H = \sum_k \psi_k^\dagger H_k \psi_k, \quad H_k = \vec{\sigma} \cdot \vec{h}(k,t), \tag{2}$$

where $\vec{\sigma} = (\sigma_x, \sigma_y, \sigma_z)$ denotes the standard Pauli matrices, k is the wave vector with $\hbar k$ being the momentum, and $\vec{h}(k,t) = (h_x(k,t), h_y(k,t), h_z(k,t))^T$ is the Hamiltonian density in momentum space. The time dependence of $\vec{h}(k,t)$ is fixed by the drive; in this paper, we shall consider the case where the drive is characterized by a time period $T = 2\pi/\omega$, where ω is the drive frequency. In what follows, we shall consider $\psi_k = (a_k, b_k)^T$ to be a two-component fermionic field characterized by annihilation operators a_k and b_k. The exact nature of these operators depend on the model and shall be discussed in detail in subsequent sections for the SSH and the Ising models.

The unitary evolution operator for such systems can be expressed in term of their Floquet Hamiltonian

$$U(T,0) = \prod_k U_k(T,0) = T_t e^{-i\int_0^T dt H(t)/\hbar} = e^{-iH_F T/\hbar}, \tag{3}$$

where H_F is the Floquet Hamiltonian of the system. Thus, U_k for such models can be resolved in terms of the Floquet eigenvalues and eigenvectors. Since $U_k(T,0)$ is a 2×2 matrix, we find

$$U_k(T,0) = \sum_{j=1,2} e^{-i\epsilon_F^{(j)}(k)T/\hbar} |n_j(k)\rangle\langle n_j(k)|, \tag{4}$$

where $\epsilon_F^{(j)}(k)$, for $j = 1, 2$, are the Floquet eigenvalues and $|n_j(k)\rangle$ are the corresponding eigenvectors.

To compute the correlation functions for such a driven system, we start from an initial state $|\psi_k^{\text{in}}\rangle$ and compute the expectation value

$$C_k(nT) = \langle \psi_k^{\text{in}} | (U_k^\dagger)^n O_k (U_k)^n | \psi_k^{\text{in}} \rangle, \tag{5}$$

where O_k is a generic quadratic operator constructed out of ψ_k and $\psi_k^\dagger$. The specific forms of these operators shall be discussed in subsequent sections in the context of the SSH and Ising models. We note that for the integrable models treated here, the correlations of O_k constitute the most general independent correlation functions; all quartic or higher order correlation of fermionic operators can be expressed in terms of O_k.

Using Eq. (4), we can express these correlations as

$$\begin{aligned} C_k(nT) &= C_{0k} + \delta C_k(nT), \\ C_{0k} &= \sum_j |\alpha_j(k)|^2 O_{jj}(k), \\ \delta C_k(nT) &= e^{-in\Delta(k)T/\hbar} f(k) + \text{H.c.}, \\ f(k) &= \alpha_2^*(k)\alpha_1(k) O_{12}(k), \\ C_x(nT) &= \int_{\text{BZ}} \frac{dk}{2\pi} e^{ikx} C_k(nT), \end{aligned} \tag{6}$$

where the integral is taken over the Brillouin zone. Here the Floquet energy gap $\Delta(k)$, the overlap $\alpha_j(k)$ of the initial state with the Floquet eigenstates, and the matrix elements $O_{j_1 j_2}(k)$ are given by

$$\begin{aligned} &\Delta(k) = \epsilon_F^{(1)}(k) - \epsilon_F^{(2)}(k), \quad \alpha_j(k) = \langle \psi_k^{\text{in}} | n_j(k) \rangle, \\ &O_{j_1 j_2}(k) = \langle n_{j_1}(k) | O_k | n_{j_2}(k) \rangle. \end{aligned} \tag{7}$$

We note that the Fourier transform of C_{0k} [Eqs. (6)] denotes the steady-state value of C_x in real space which is independent of n. Thus,

$$\delta C_x(nT) = \int_{\text{BZ}} \frac{dk}{2\pi} e^{ikx} (f(k) e^{-in\Delta(k)T/\hbar} + \text{H.c.}) \tag{8}$$

represents the deviation of $C_x(nT)$ from its steady-state value in real space. Since such a steady state is reached for large n in any driven system, we expect $\delta C_x(nT)$ to be a decaying function of n for large n.

To understand the nature of this decay, we note that for large n, the integral for $\delta C_x(nT)$ can be evaluated within a stationary point approximation. To this end, let us assume that the leading contribution to the integral comes from a stationary point at $k = k_0$. Around this point, let us assume that

$$\begin{aligned} &\Delta(k) \simeq \Delta(k_0) + \Delta^{(\beta)}(k_0)\delta k^\beta + \cdots, \\ &f(k) \simeq f(k_0) + f^\alpha(k_0)\delta k^\alpha + \cdots, \\ &\Delta^{(\beta)}(k_0) = \frac{1}{\beta!} \frac{\partial^\beta \Delta(k)}{\partial k^\beta}\Big|_{k=k_0}, \quad f^\alpha(k_0) = \frac{1}{\alpha!} \frac{\partial^\alpha f(k)}{\partial k^\alpha}\Big|_{k=k_0}, \end{aligned} \tag{9}$$

where α and β denote the leading powers for expansion $\Delta(k)$ and $f(k)$, respectively, around $k = k_0$. We note that since k_0 is a stationary point, $\beta \geqslant 2$. Substituting Eqs. (9) in Eq. (8), we find the leading behavior of the correlation to be given by

$$\begin{aligned} \delta C_x(nT) \sim A(k_0; n, T) \int_{-\infty}^{\infty} \frac{d\delta k}{2\pi} e^{i\delta k x} \big(f^\alpha(k_0)\delta k^\alpha \\ \times e^{-in\Delta^{(\beta)}(k_0)\delta k^\beta T/\hbar} \big) + \text{H.c.}, \end{aligned} \tag{10}$$

where we have included $f(k_0) \equiv f^{(0)}(k_0)$ by allowing the exponent α to have zero value. Here $A(k_0; n, T) = \exp[i(k_0 x - \Delta(k_0)nT)]$ is a phase factor which does not contribute to the decay of the correlator since its an oscillatory function of n. A scaling $\delta k \to \delta k' = n^{1/\beta}\delta k$ and $x \to x' = x/n^{1/\beta}$ in the integral in Eq. (10) leads to

$$\begin{aligned} \delta C_x(nT) &= A(k_0; n, T) n^{-(\alpha+1)/\beta} g(k_0; x') + \text{H.c.}, \\ g(k_0; z) &= \int_{-\infty}^{\infty} \frac{dy}{2\pi} f^\alpha(k_0) y^\alpha e^{i(yz - \Delta^{(\beta)}(k_0) y^\beta T/\hbar)}. \end{aligned} \tag{11}$$

Since $g(k_0; z)$ is an oscillatory function of z, it does not contribute to the decay of the correlators. Thus, we find the general result that the leading decay of the correlator is given by

$$C_x(nT) \sim n^{-(\alpha+1)/\beta}, \tag{12}$$

which is the main result of this section. For multiple stationary points, it is easy to see that the leading behavior is given by the one which allows for the slowest decay.

We note that for any stationary point expansion, generically, we expect $\beta = 2$ since the second derivative of the energy gap need not vanish at the stationary point. In this case, we find that the correlators would decay as $\delta C_x(nT) \sim n^{-3/2}$ if $f(k_0)$ vanishes at the point and $f(k_0 + \delta k) \sim (\delta k)^2$ as $\delta k \to 0$ and as $\delta C_x(nT) \sim n^{-1/2}$ if $f(k_0)$ is finite (this corresponds to $\alpha = 0$). These two behaviors correspond to two dynamical phases; the former behavior is seen for high drive frequencies where the stationary point typically occurs at the edge of the Brillouin zone [46], while the latter occurs at lower frequencies where additional stationary points which correspond to $\alpha = 0$ appear inside the Brillouin zone. As noted in Ref. [46], these two phases are separated by a dynamical phase transition characterized by a critical drive frequency ω_c.

The decay of the correlators exactly at the transition allows for richer behavior, which we explore next. We note that exactly at the transition point, the Floquet energy gap $\Delta(k)$ must have a point of inflection which necessitates its second derivative to also vanish. Thus, for this case $\beta > 2$. Depending on the symmetry of model, we find that either the third or fourth derivative of the Floquet gap contributes to the lowest nonvanishing term in the expansion of $\Delta(k)$ about $k = k_0$. The former behavior corresponds to $\beta = 3$ and occurs if the Floquet energy is odd under the transformation $k \to -k$. This leads to

$$C_x(nT) \sim n^{-(\alpha+1)/3}. \tag{13}$$

In contrast, if the Floquet energy is even under $k \to -k$, its fourth derivative contributes to the lowest nonvanishing term. This yields $\beta = 4$ and leads to

$$C_x(nT) \sim n^{-(\alpha+1)/4}. \tag{14}$$

Thus the decay of the correlators may follow a different power law at the critical point. Such a point may separate two distinct dynamical phases characterized by different values of α; however, this is not a necessary condition for the existence of a critical frequency where the decay exponent changes. Indeed, as we shall see in Sec. III, one may have such points at a frequency $\omega = \omega_c$ with same α for both $\omega > \omega_c$ and $\omega < \omega_c$. This is possible since β (and hence ω_c) is determined by the property of the Floquet quasienergy gap while $f(k)$ (and thus α) depends on the operator whose correlation is measured. We note that a special case of the general results given by Eq. (14) for $\alpha = 2$ and $\beta = 4$ leading to $n^{-3/4}$ decay has been found earlier in Ref. [49].

Finally, we discuss the crossover scale n_c which denotes the number of drive cycles after which the system crosses over to a decay characterized by $\beta = 2$. We note that n_c diverges at a dynamical transition and tends to zero far away from it. To

estimate n_c, we note that near a transition we can always write

$$\delta C_x(nT) \sim A(k_0; n, T) \int_{-\infty}^{\infty} \frac{d\delta k}{2\pi} e^{-i\delta k x} \times \left(f^{\alpha}(k_0) \delta k^{\alpha} e^{-in(c_1 \delta k^{a_0} + c_2 \delta k^{\beta_0} + \ldots)T/\hbar} \right) + \text{H.c.}, \quad (15)$$

where c_1 and c_2 are the coefficients of expansions of the Floquet spectrum around $k = k_0$, β_0 denotes the lowest integer larger than a_0 for which $c_2 \neq 0$, $a_0 = 1$ or 2 depending on the symmetry of the Floquet spectrum, and the ellipsis indicates higher order terms in the expansion of $\Delta(k)$ around $k = k_0$ which we shall ignore. Note that here we approach the transition from one of the dynamic phases; the exponent α corresponding to $f(k)$ remains the same since we do not cross the transition. A simple scaling $k \to \delta k' = n^{1/\beta_0} \delta k$ yields

$$\delta C_x(nT) \sim A(k_0; n, T) \int_{-\infty}^{\infty} \frac{d\delta k'}{2\pi} e^{-i\delta k' n^{1/\beta_0} x} \times \left[f^{\alpha}(k_0) n^{-(\alpha+1)/\beta_0} (\delta k')^{\alpha} \times e^{-i(c_1 n^{1-a_0/\beta_0} (\delta k')^{a_0} + c_2 (\delta k')^{\beta_0})T/\hbar} + \text{H.c.} \right]. \quad (16)$$

Thus, the behavior of the integral is governed by the coefficient of $(\delta k')^{a_0}$ in the exponent after

$$n_c \simeq (c_2/c_1)^{\beta_0/(\beta_0 - a_0)} \quad (17)$$

drive cycles. Hence, the crossover scale is also controlled by the symmetry of the model which renders $a_0 = 1(2)$ and $\beta_0 = 3(4)$ for models whose Floquet spectrum is odd (even) under $k \to -k$ near the transition point. Furthermore, for a generic transition point for these integrable models, $c_1 \sim |\omega - \omega_c|$ and c_2 is a constant. Thus we find

$$n_c \sim |\omega - \omega_c|^{-\beta_0/(\beta_0 - a_0)}, \quad (18)$$

which shows that n_c diverges at the transition point where $c_1 = 0$ and is small away from the transition where generically $c_1 \ll c_2$. We explore this crossover physics in detail in Secs. III and IV in the context of specific models.

III. SSH MODEL

In this section, we will study the effect of periodic driving in the Su-Schrieffer-Heeger (SSH) model. We will show that the long-time behavior of the correlation function can show transitions between different power laws for some special choices of the driving parameters. We shall analyze the driven SSH model within first-order FPT; this is done so as to obtain simple analytical insights. The results obtained from FPT shall be compared with exact numerics toward the end of the section.

The SSH model is a tight-binding model of noninteracting electrons in 1D in which the nearest-neighbor hopping has different strengths on alternate bonds [51]. We will ignore the spin of the electron since it will not play any role in this paper. In second-quantized notation, the Hamiltonian for a system with N sites (where N is even) and periodic boundary conditions is given by

$$H = \sum_{n=1}^{N/2} [\gamma_1 a_n^{\dagger} b_n + \gamma_2 b_n^{\dagger} a_{n+1} + \text{H.c.}], \quad (19)$$

where $a_{N/2+1} \equiv a_1$. (We will set both Planck's constant $\hbar$ and the spacing a between nearest-neighbor sites to 1). Transforming to momentum space, we find that

$$H = \sum_k [\gamma_1 a_k^{\dagger} b_k + \gamma_2 b_k^{\dagger} a_k e^{i2k} + \text{H.c.}], \quad (20)$$

where k takes $N/2$ equally spaced values lying in the range $[-\pi/2, \pi/2]$. This can be written in terms of a 2×2 matrix H_k as

$$H = \sum_k (a_k^{\dagger} \quad b_k^{\dagger}) H_k \begin{pmatrix} a_k \\ b_k \end{pmatrix}, \quad H_k = \begin{pmatrix} 0 & \gamma_1 + \gamma_2 e^{-i2k} \\ \gamma_1 + \gamma_2 e^{i2k} & 0 \end{pmatrix}. \quad (21)$$

The energy-momentum dispersion is given by $E_{k\pm} = \pm E_k$, where

$$E_k = \sqrt{\gamma_1^2 + \gamma_2^2 + 2\gamma_1 \gamma_2 \cos(2k)}. \quad (22)$$

We see that the spectrum has a minimum gap equal to $E_{k+} - E_{k-} = 2|\gamma_1 \pm \gamma_2|$ at $k = 0$ and $\pm\pi/2$, respectively, depending on whether γ_1 and γ_2 have opposite signs or the same sign.

We will now consider driving this system periodically in time [54–59] by adding a term to the hopping which is of the form $a \sin(\omega t)$, where a and ω are the driving amplitude and frequency, respectively. The Hamiltonian in momentum space is therefore given by

$$H = \sum_k [(\gamma_1 + a \sin(\omega t)) a_k^{\dagger} b_k + (\gamma_2 + a \sin(\omega t)) b_k^{\dagger} a_k e^{i2k} + \text{H.c.}]. \quad (23)$$

This system can be analytically studied by several methods such as the Floquet-Magnus expansion, which works in the limit ω, is much larger than all the other parameters, a, γ_1, and γ_2, and FPT which is valid in the limit that both a and ω are much larger than γ_1 and γ_2. We will use FPT, which proceeds as follows.

For each value of k, we consider the Floquet operator

$$U_k = \mathcal{T} \exp[-i \int_0^T dt H_k(t)], \quad (24)$$

where $\mathcal{T}$ denotes time-ordering. Note that U_k is an SU(2) matrix since $H_k(t)$ is a Hermitian and traceless matrix for all times t. We can write the Floquet operator as

$$U_k = e^{-iH_{Fk}T}, \quad (25)$$

where H_{Fk} is time independent and is called the Floquet Hamiltonian. Assuming $a \gg \gamma_1, \gamma_2$, we write

$$H_k(t) = H_0(t) + V, \quad H_0(t) = \begin{pmatrix} 0 & a \sin(\omega t)(1 + e^{-i2k}) \\ a \sin(\omega t)(1 + e^{i2k}) & 0 \end{pmatrix}, \quad V = \begin{pmatrix} 0 & \gamma_1 + \gamma_2 e^{-i2k} \\ \gamma_1 + \gamma_2 e^{i2k} & 0 \end{pmatrix}. \quad (26)$$

We will find the form of H_{Fk} only to first order in the perturbation V.

The instantaneous eigenvalues of $H_0(t)$ are given by $E_{k+} = 2a\sin(\omega t)\cos k$ and $E_{k-} = -2a\sin(\omega t)\cos k$. These satisfy the condition

$$e^{i\int_0^T dt(E_{k+}-E_{k-})} = 1. \tag{27}$$

We will therefore have to carry out degenerate FPT. The eigenfunctions corresponding to $E_{k\pm}$ are given by

$$|+\rangle_k = \frac{1}{\sqrt{2}}\begin{pmatrix}1\\ e^{ik}\end{pmatrix},$$
$$|-\rangle_k = \frac{1}{\sqrt{2}}\begin{pmatrix}1\\ -e^{ik}\end{pmatrix}. \tag{28}$$

We begin with the Schrödinger equation

$$i\frac{d|\psi\rangle}{dt} = (H_0 + V)|\psi\rangle. \tag{29}$$

We assume that $|\psi(t)\rangle$ has the expansion

$$|\psi(t)\rangle = \sum_n c_n(t)\, e^{-i\int_0^t dt' E_n(t')}|n\rangle, \tag{30}$$

where $|n\rangle = |+\rangle$ and $|-\rangle$. Equation (29) then implies that

$$\frac{dc_m}{dt} = -i\sum_n \langle m|V|n\rangle e^{i\int_0^t dt'(E_m(t')-E_n(t'))}c_n. \tag{31}$$

Integrating this equation, and keeping terms only to first order in V, we find that

$$c_m(T) = c_m(0) \; - \; i\sum_n \int_0^T dt\,\langle m|V|n\rangle \times e^{i\int_0^t (E_m(t')-E_n(t'))\,dt'} c_n(0). \tag{32}$$

This can be written as

$$c_m(T) \; = \; \sum_n \left(I - iH_{Fk}^{(1)}T\right)_{mn} c_n(0), \tag{33}$$

where I denotes the identity matrix and $H_F^{(1)}$ is the Floquet Hamiltonian to first order in V. We then find, using the identity $e^{iz\sin x} = \sum_{n=-\infty}^{\infty} J_n(z)e^{inx}$ (where J_n denotes the n^{th} order Bessel function), that

$$\langle +|H_{Fk}^{(1)}|+\rangle = (\gamma_1+\gamma_2)\cos k,$$
$$\langle -|H_{Fk}^{(1)}|-\rangle = -(\gamma_1+\gamma_2)\cos k,$$
$$\langle +|H_{Fk}^{(1)}|-\rangle = -i(\gamma_1-\gamma_2)(\sin k)J_0\left(\frac{4a}{\omega}\cos k\right)e^{i\frac{4a}{\omega}\cos k},$$
$$\langle -|H_{Fk}^{(1)}|+\rangle = i(\gamma_1-\gamma_2)(\sin k)J_0\left(\frac{4a}{\omega}\cos k\right)e^{-i\frac{4a}{\omega}\cos k}. \tag{34}$$

$H_{Fk}^{(1)}$ then takes the following form in the $|+\rangle_k,\ |-\rangle_k$ basis:

$$H_{Fk}^{(1)} = (\gamma_1+\gamma_2)\cos k\,\sigma_z + (\gamma_1-\gamma_2)(\sin k)J_0\left(\frac{4a}{\omega}\cos k\right)\sin\left(\frac{4a}{\omega}\cos k\right)\sigma_x + (\gamma_1-\gamma_2)(\sin k)J_0\left(\frac{4a}{\omega}\cos k\right)\cos\left(\frac{4a}{\omega}\cos k\right)\sigma_y. \tag{35}$$

We now change the basis to

$$|\uparrow\rangle_k = a_k^\dagger|0\rangle,$$
$$|\downarrow\rangle_k = b_k^\dagger|0\rangle, \tag{36}$$

so

$$|+\rangle_k = \frac{1}{\sqrt{2}}(|\uparrow\rangle_k + e^{ik}|\downarrow\rangle_k),$$
$$|-\rangle_k = \frac{1}{\sqrt{2}}(|\uparrow\rangle_k - e^{ik}|\downarrow\rangle_k). \tag{37}$$

In the $|\uparrow\rangle_k, |\downarrow\rangle_k$ basis, we get

$$H_{Fk}^{(1)} = \left[(\gamma_1+\gamma_2)\cos^2 k + (\gamma_1-\gamma_2)J_0\left(\frac{4a}{\omega}\cos k\right)\cos\left(\frac{4a}{\omega}\cos k\right)\sin^2 k\right]\sigma_x + \sin k\cos k\left[(\gamma_1+\gamma_2) - (\gamma_1-\gamma_2)J_0\left(\frac{4a}{\omega}\cos k\right)\cos\left(\frac{4a}{\omega}\cos k\right)\right]\sigma_y + (\gamma_1-\gamma_2)(\sin k)J_0\left(\frac{4a}{\omega}\cos k\right)\sin\left(\frac{4a}{\omega}\cos k\right)\sigma_z. \tag{38}$$

Before proceeding further, we make two comments about the exact form of H_{Fk} to all orders based on certain symmetries. First, H_{Fk} must be an odd function of $\gamma_1,\ \gamma_2$. To see this, we note that Eq. (24) can be written as a product of N_t factors in which t increases from 0 to T as we go from right to left in steps of T/N_t (eventually, we take the limit $N_t \to \infty$). We then use the fact that the driving term satisfies $\sin(\omega(T-t)) = -\sin(\omega t)$ to see that

$$[U_k(\gamma_1,\gamma_2)]^{-1} = U_k(-\gamma_1,-\gamma_2), \tag{39}$$

if we hold $a,\ \omega$ fixed. Equation (25) then implies that

$$H_F(-\gamma_1,-\gamma_2) = -H_F(\gamma_1,\gamma_2). \tag{40}$$

Hence H_F can only have odd powers of $\gamma_1,\ \gamma_2$. This implies that if $\gamma_1, \gamma_2 \ll a, \omega$, the first-order Floquet Hamiltonian will be a very good approximation to the exact Floquet Hamiltonian since the next correction is of third order in $\gamma_1,\ \gamma_2$. Second, let us consider the special case $\gamma_2 = -\gamma_1$ which will be considered in more detail below. We then find that after doing a unitary transformation,

$$H_k(t) \to V_k H_k(t) V_k^\dagger,$$
$$\text{where} \quad V_k \; = \; \begin{pmatrix}1 & 0\\ 0 & e^{-ik}\end{pmatrix}, \tag{41}$$

we obtain

$$H_k(t) = 2a\sin(\omega t)\cos k\sigma_x - 2\gamma_1\sin k\sigma_y. \tag{42}$$

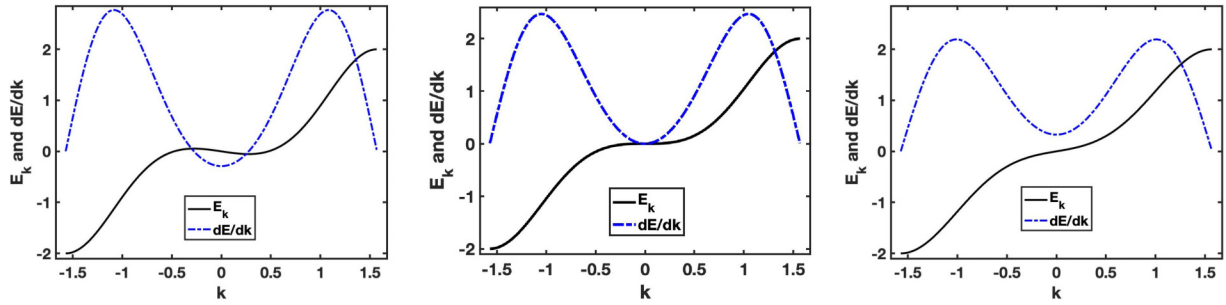

FIG. 1. Energy E_k (black solid line) and its first derivative dE_k/dk (blue dot-dashed line) versus k obtained from the first-order Floquet Hamiltonian for $\gamma_1 = 1,\ \gamma_2 = -1,\ a = 6$, and (left panel) $\omega = 4a/(\mu_1 + 0.3)$, (middle panel) $\omega = 4a/\mu_1$, and (right panel) $\omega = 4a/(\mu_1 - 0.3)$. For $\omega = 4a/\mu_1$, there is a stationary point at $k = 0$ with both dE_k/dk and d^2E_k/dk^2 equal to zero.

We now use Eq. (42) to calculate the Floquet operator and Floquet Hamiltonian in Eqs. (24) and (25). Then an argument similar to the one above shows that

$$[U_k]^{-1} = U_{-k}, \tag{43}$$

where we have held $\gamma_1,\ \gamma_2$ fixed and only changed $k \to -k$. Equation (43) implies that

$$H_{F,-k} = -H_{F,k}. \tag{44}$$

This means that the eigenvalues of H_F (quasienergies) must be odd functions of k if $\gamma_2 = -\gamma_1$.

The eigenvalues of the first-order Floquet Hamiltonian in Eq. (38) are given by $\pm E_k$ [with the Floquet energy gap being $\Delta(k) = 2E(k)$], where

$$E_k = \sqrt{(\gamma_1+\gamma_2)^2\cos^2 k + (\gamma_1-\gamma_2)^2\sin^2 k\left[J_0\left(\frac{4a}{\omega}\cos k\right)\right]^2}. \tag{45}$$

For general values of $\gamma_1,\ \gamma_2$, we see that E_k is nonzero for all values of k. However, for $\gamma_2 = \gamma_1$ it vanishes if $k = \pi/2$ (in fact, E_k does not depend on the driving if $\gamma_2 = \gamma_1$), while for $\gamma_2 = -\gamma_1$ it vanishes when either $k = 0$ or $J_0((4a/\omega)\cos k) = 0$. Thus, driving can lead to nontrivial zeros of the Floquet energy for special values of $(a/\omega)\cos k$. In the rest of this section, we will therefore consider the case $\gamma_2 = -\gamma_1$. Setting $\gamma_1 = 1$, we have

$$E_k = 2(\sin k)J_0\left(\frac{4a}{\omega}\cos k\right). \tag{46}$$

Figure 1 shows plots of E_k and dE_k/dk for a system with $\gamma_1 = 1,\ \gamma_2 = -1,\ a = 6$, and $\omega < \omega_c$, $\omega = \omega_c$ and $\omega > \omega_c$, where $\omega_c = 4a/\mu_1$ and $\mu_1 \simeq 2.4048$ is the first zero of $J_0(z)$. At $k = 0$, we see that $E_k = 0$ in all three cases, but $dE_k/dk = 0$ only if $\omega = \omega_c$.

While the calculations shown above are for the case of a driving of the form $a\sin(\omega t)$, it turns out that the expressions for the Floquet Hamiltonian and therefore its eigenvectors simplify considerably when the driving is given by $a\cos(\omega t)$. We then find that

$$H_{Fk}^{(1)} = \left[(\gamma_1+\gamma_2)\cos^2 k + (\gamma_1-\gamma_2)J_0\left(\frac{4a}{\omega}\cos k\right)\sin^2 k\right]\sigma_x + \sin k\cos k\left[(\gamma_1+\gamma_2) - (\gamma_1-\gamma_2)J_0\left(\frac{4a}{\omega}\cos k\right)\right]\sigma_y. \tag{47}$$

We will consider this driving in the rest of the section for both analytical and numerical studies. Note that the eigenvalues of the Floquet operator and hence of the Floquet Hamiltonian ($\pm E_k$) are independent of the phase of the driving, i.e., they do not depend on ϕ when the driving is $a\sin(\omega t + \phi)$. We will see that the analysis in the rest of this section is governed mainly by the properties of E_k and we can therefore choose any value of ϕ for our calculations.

We now consider an operator of the form $a_j^\dagger b_j$ where j denotes a particular unit cell. Starting from an initial state $\Psi(0)$, we will look at the correlation function at stroboscopic instances of time $t = nT$,

$$C_n = \langle\Psi(nT)|a_j^\dagger b_j|\Psi(nT)\rangle, \tag{48}$$

and we will study how this behaves for large values of n. We take the initial state to be a half-filled state given by a product in momentum space:

$$|\Psi(0)\rangle = \prod_k [(a_k^\dagger + e^{i\phi}b_k^\dagger)/\sqrt{2}]|\text{vac}\rangle. \tag{49}$$

For simplicity, we have taken the phase ϕ to be independent of k:

$$\begin{aligned} C_n &= \frac{2}{N}\sum_k \langle\Psi(nT)|a_k^\dagger b_k|\Psi(nT)\rangle \\ &= \frac{2}{N}\sum_k \langle\Psi(0)|(U_k^\dagger)^n a_k^\dagger b_k (U_k)^n|\Psi(0)\rangle. \end{aligned} \tag{50}$$

$H_{Fk}^{(1)}$ can be written in the following matrix form:

$$H_{Fk}^{(1)} = E_k\begin{pmatrix} 0 & ie^{-ik} \\ -ie^{ik} & 0 \end{pmatrix}, \tag{51}$$

whose eigenvalues are $\pm E_k$ and eigenfunctions are

$$|+\rangle_k = \frac{1}{\sqrt{2}}\begin{pmatrix}1\\ -ie^{ik}\end{pmatrix},$$
$$|-\rangle_k = \frac{1}{\sqrt{2}}\begin{pmatrix}1\\ ie^{ik}\end{pmatrix}. \tag{52}$$

Then we have

$$(U_k)^n = e^{-inE_kT}|+\rangle_k\langle+|_k + e^{inE_kT}|-\rangle_k\langle-|_k.$$
$$= \begin{pmatrix}\cos(nE_kT) & e^{-ik}\sin(nE_kT)\\ -e^{ik}\sin(nE_kT) & \cos(nE_kT)\end{pmatrix}. \tag{53}$$

Since

$$a_k^\dagger|\text{vac}\rangle = \begin{pmatrix}1\\0\end{pmatrix}, \quad b_k^\dagger|\text{vac}\rangle = \begin{pmatrix}0\\1\end{pmatrix}, \tag{54}$$

we find that

$$(U_k^\dagger)^n a_k^\dagger b_k (U_k)^n = \begin{pmatrix}-\frac{1}{2}e^{ik}\sin(2nE_kT) & \cos^2(nE_kT)\\ -e^{i2k}\sin^2(nE_kT) & \frac{1}{2}e^{ik}\sin(2nE_kT)\end{pmatrix}. \tag{55}$$

Using Eqs. (49) and (55), we obtain

$$C_n = A + \frac{2}{N}\sum_k f(k)\cos(2nTE_k),$$
$$A = \frac{1}{2N}\sum_k (e^{i\phi} - e^{i(2k-\phi)}),$$
$$f(k) = \frac{1}{4}(e^{i\phi} + e^{i(2k-\phi)}). \tag{56}$$

For $N \to \infty$, these quantities have the integral forms

$$C_n = A + \frac{1}{4\pi}\int_{-\pi/2}^{\pi/2} dk\,(e^{i\phi} + e^{-i\phi}\cos(2k))\cos(2nTE_k),$$
$$A = \frac{1}{4\pi}\int_{-\pi/2}^{\pi/2} dk\,(e^{i\phi} - e^{i(2k-\phi)}) = \frac{e^{i\phi}}{4}, \tag{57}$$

where we have used the relation $\cos(2nTE_k) = \cos(2nTE_{-k})$ (since $E_{-k} = -E_k$) to write the first equation in Eq. (57).

We will now study the form of the n-dependent part of C_n, called δC_n, for large n. The dominant contributions will come from regions around the values of k where E_k has an extremum, namely, $dE_k/dk = 0$. One such point is $k = \pi/2$. Expanding around it to second order, we find that $E_k = 2 - (1 + 8a^2/\omega^2)(k - \pi/2)^2$, where we have used the expansion $J_0(z) = 1 - z^2/4$ for small z. We first assume that $f(k = \pi/2) \neq 0$; this will be true if ϕ is not an integer multiple of π. Near $k' = k - \pi/2$, the n-dependent term in Eqs. (57) then takes the form

$$\delta C_n \simeq \frac{i}{2\pi}\int dk'\ \sin\phi\ \text{Re}$$
$$\times\ \exp[i4nT - i2nT(1 + 8a^2/\omega^2)k'^2], \tag{58}$$

where Re denotes the real part. We thus see that C_n will oscillate as $\cos(4nT)$ (which implies that its absolute value will vary periodically with n with a period $\Delta n = \pi/(4T) = \omega/8$) multiplied by an integral of the form $\int dk' \exp[i\alpha n k'^2]$ which, by a scaling argument, will decay as $1/n^{1/2}$ for large n. However, in the special case that ϕ is an integer multiple of π, both $e^{i\phi} + e^{-i\phi}\cos(2k)$ and its first derivative vanish at $k = \pi/2$. We then get a factor of k'^2 appearing in the integrand of Eq. (58). The integral will therefore be of the form $\int dk' k'^2 \exp[i\alpha n k'^2]$, which will decay as $1/n^{3/2}$ for large n. Below we will see plots showing a $1/n^{1/2}$ decay (for $\phi = \pi/4$; Fig. 2) and a $1/n^{3/2}$ decay (for $\phi = 0$; Fig. 5).

Next, we consider if there are any other values of k where $dE_k/dk = 0$. We find that such points exist if $\omega < \omega_c$, where $\omega_c = 4a/\mu_1$. This is because, as k goes from 0 to $\pi/2$, $\sin k$ goes from 0 to 1, taking only positive values in between, while $J_0((4a/\omega)\cos k)$ goes between $J_0(4a/\omega)$ and 1, crossing zero p times in between if $4a/\omega$ is larger than the first p zeros of $J_0(z)$. This implies that E_k in Eq. (46) will go between 0 and 2, crossing zero p times in between; hence E_k will have p extrema where $dE_k/dk = 0$. Next, if $k = k_0$ is one of the points where $dE_k/dk = 0$, and k_0 is not equal to either 0 or $\pi/2$, the factor $f(k)$ in Eq. (48) is not zero, but the argument of $\cos(2E_k nT)$ will go as $\cos(2E_{k_0}nT + \alpha n(k - k_0)^2)$. This means that δC_n will oscillate as $\cos(2E_{k_0}nT)$ (implying that its absolute value with vary periodically with a period $\Delta n = \omega/(4E_{k_0})$) multiplied by an integral of the form $\int dk' \exp[i\alpha n k'^2]$. By a scaling argument, this will again decay as $1/n^{1/2}$ for large n.

We thus conclude that δC_n will generally oscillate and decay as $1/n^{1/2}$. This is what we see in Fig. 2, left and middle panels, for a system with $\gamma_1 = 1$, $\gamma_2 = -1$, $a = 6$, $\omega = 4a/(\mu_1 \pm \epsilon)$, where $\epsilon = 0.1$, and $\phi = \pi/4$ for the initial state [see Eq. (49)]. If $4a/\omega$ is larger than p zeros of $J_0(z)$ (where p can be $1, 2, 3, \cdots$), there will be p terms in δC_n, all of which decay as $1/n^{1/2}$ but which oscillate with p different periods Δn.

Interestingly, a different scaling of δC_n versus n arises if ω is exactly equal to $\omega_p = 4a/\mu_p$ with μ_p being the pth zero of $J_0(z)$. (We will call the ω_p's critical frequencies, ω_1 being the largest such frequency). Then both E_k and its first two derivatives vanish at $k = 0$ as we will now show. For definiteness, we consider the neighborhood of ω_1, namely, we take $\omega = 4a/(\mu_1 + \epsilon)$, where $|\epsilon| \ll 1$. We now expand Eq. (46) around $k = 0$ up to order k^3. Using the property $dJ_0(z)/dz = -J_1(z)$ and $J_1(\mu_1) \equiv \nu_1 \simeq 0.519$, we find that

$$E_k \simeq \nu_1(-2\epsilon k + \mu_1 k^3). \tag{59}$$

Equation (48) then gives, in the region around $k = 0$,

$$\delta C_n \simeq \frac{\cos\phi}{2\pi}\int dk \text{Re}\exp[i2nT\,\nu_1(-2\epsilon k + \mu_1 k^3)]. \tag{60}$$

Defining a scaled variable $k' = kn^{1/3}$, we get

$$\delta C_n \simeq \frac{\cos\phi}{2\pi n^{1/3}}\int dk'\ \text{Re}$$
$$\times\ \exp[i2T\ \nu_1\ (-2\epsilon n^{2/3}k'\ +\ \mu_1 k'^3)]. \tag{61}$$

We see from Eq. (61) that if $\epsilon = 0$, i.e., $\omega = \omega_1$ exactly, δC_n will go as $1/n^{1/3}$ times a factor which does not oscillate with n at large n. This can be seen in Fig. 2, right panel. (If n is not very large, we see some oscillations which arise due to the stationary point at $k = \pi/2$). Further, if ϵ is nonzero but small, then we will still get the $1/n^{1/3}$ scaling if $|\epsilon|n^{2/3} \ll 1$ since the term of order k' will dominate over the term of order k'^3. But

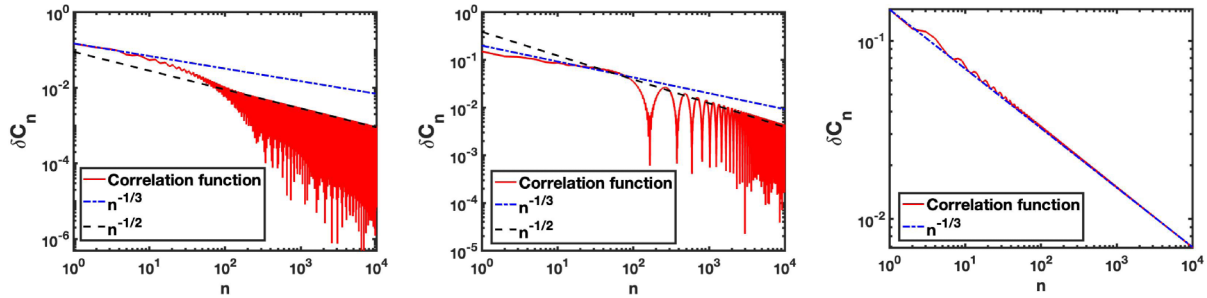

FIG. 2. Log-log plots of the absolute value of the n-dependent part δC_n of the correlation function $\langle a_j^\dagger b_j \rangle$ as a function of the time nT, for $\gamma_1 = 1$, $\gamma_2 = -1$, $a = 6$, $\omega = 4a/(\mu_1 + \epsilon)$, and $\phi = \pi/4$ for the initial state. Here μ_1 denotes the first zero of the Bessel function J_0 so $\omega_c = 4a/\mu_1$ is the critical frequency. Left panel: $\epsilon = -0.1$, so $\omega > \omega_c$. Middle panel: $\epsilon = 0.1$, hence $\omega < \omega_c$. Right panel: $\epsilon = 0$, hence $\omega = \omega_c$. Both the left and middle panels show crossovers between $1/n^{1/3}$ and an oscillating function times $1/n^{1/2}$. The right panel with $\epsilon = 0$ and hence $\omega = \omega_c$ shows only a $1/n^{1/3}$ scaling with no oscillations.

if $|\epsilon| n^{2/3} \gg 1$, the k' term will dominate over the k'^3 term, and we do not expect to get the $1/n^{1/3}$ scaling anymore. We will then get the other scaling, namely, an oscillating function of n times $1/n^{1/2}$. Hence, a crossover will occur between a nonoscillating function of n times $1/n^{1/3}$ and an oscillating function of n times $1/n^{1/2}$ at a crossover n_c which scales with ϵ as $1/|\epsilon|^{3/2}$. This is shown in Fig. 3. Since $|\epsilon| \sim |\omega - \omega_1|$, we see that $n_c \sim 1/|\omega - \omega_1|^{3/2}$. This corresponds to $\beta_0 = 3$ and $a_0 = 1$ [Eq. (18)].

We now consider the oscillations which appear in δC_n when n is larger than the crossover scale and ω not equal to a critical frequency. These are shown in Fig. 2, left and middle panels, for ω close to the value $4a/\mu_1$. For $\epsilon < 0$, $|\delta C_n|$ goes as an oscillating function of n times $1/n^{1/2}$ due to the integral over the region around $k = \pi/2$; the oscillation period is $\Delta n = \omega/8$ which is independent of ϵ and too small to be visible in Fig. 2, left panel. But for $\epsilon > 0$, we see in Fig. 2, middle panel, that the oscillations in δC_n have quite a large

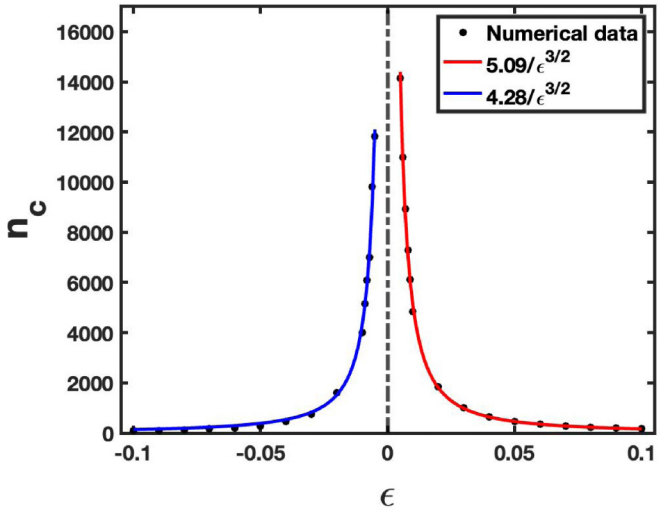

FIG. 3. Plot of crossover scale n_c versus ϵ, for $\gamma_1 = 1$, $\gamma_2 = -1$, $a = 6$, $\omega = 4a/(\mu_1 + \epsilon)$, and $\phi = \pi/4$ for the initial state. We take n_c as the point where the guiding line for $1/n^{1/2}$ behavior (black dashed line) first crosses the numerical result in the left panel of Fig. 2 and where the first large dip in the correlation function appears in the middle panel of Fig. 2. We find that n_c diverges as $1/|\epsilon|^{3/2}$ as $\epsilon \to 0$.

period, about $\Delta n = 215$. We will now derive this. For $\epsilon > 0$, we see from Eq. (59) that $dE_k/dk = 0$ at $k = \pm k_0$, where

$$k_0 = \sqrt{\frac{2\epsilon}{3\mu_1}}. \tag{62}$$

Expanding around the stationary point at k_0, we find that the argument of the exponential in Eq. (60) is given by

$$-i2nT\nu_1 \frac{4}{3}\sqrt{\frac{2}{3\mu_1}}\epsilon^{3/2} + \text{atermoforder}(k - k_0)^2. \tag{63}$$

The Gaussian integral involving the term of order $(k - k_0)^2$ will give a scaling like $1/n^{1/2}$ while the first term in Eq. (63) implies that $|\delta C_n|$ will oscillate with n with period

$$\Delta n = \frac{\pi}{(4/3)\, 2T\, \nu_1 \sqrt{\frac{2}{3\mu_1}}\, \epsilon^{3/2}} = \frac{a}{(4/3)\, \mu_1 \nu_1 \sqrt{\frac{2}{3\mu_1}}\, \epsilon^{3/2}}, \tag{64}$$

where we have used $T = 2\pi/\omega = \pi\mu_1/(2a)$ to derive the second line. In Fig. 4, we show a plot of Δn versus ϵ, for $\gamma_1 = 1$, $\gamma_2 = -1$, $a = 6$, $\omega = 4a/(\mu_1 + \epsilon)$ for $\epsilon > 0$ (so $\omega < 4a/\mu_1$), and $\phi = \pi/4$ for the initial state. The best fit is given by $\Delta n = 6.81/\epsilon^{3/2}$, which agrees well with the value of $6.85/\epsilon^{3/2}$ that we find from Eq. (64).

Finally, we compare our results for first-order FPT with that found from exact numerics. The latter is shown in Fig. 5 for $\gamma_1 = -\gamma_2 = 1$ and $a = 6$. We note that for these values of a, γ_1, and γ_2, the first-order FPT yields a critical drive frequency to be $\omega_c \simeq 9.9799$ whereas the exact numerics leads to $\omega_c \simeq 9.9794$; this reflects the accuracy of FPT for these parameters. (This occurs since the expansion parameter for FPT is $\gamma_1/a = 1/6$ and only odd powers of this parameter appear. So the third-order term is about 36 times smaller than the first-order term). The top left panel of Fig. 5 displays the Floquet energy and its derivative as a function of k, showing that the exact Floquet energies precisely match the results from first-order FPT shown in the middle panel of Fig. 1. The top right (bottom left) panel indicates that the crossover from $n^{-1/3}$ to $n^{-1/2}(n^{-3/2})$ behavior at $\omega = 4a/(2.4048 + (-)0.1)$ is present in the exact theory and is almost identical to that

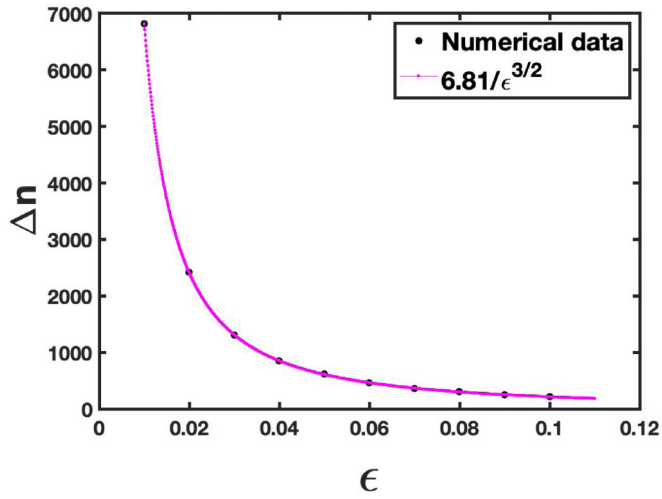

FIG. 4. Plot of oscillation period Δn versus ϵ, for $\gamma_1 = 1$, $\gamma_2 = -1$, $a = 6$, $\omega = 4a/(\mu_1 + \epsilon)$, and $\phi = \pi/4$ for the initial state. We find that Δn diverges as $1/|\epsilon|^{3/2}$ as $\epsilon \to 0$ from the positive side.

obtained within first-order FPT. Finally, the bottom right panel shows that the $n^{-1/3}$ decay of the correlation function at $\omega = \omega_c = 9.7994$ is reproduced within exact numerics. The reason for this near-exact match can be traced to a large value of a which shifts the transition to high frequency where first-order FPT naturally produces accurate results.

We end this section by noting that it is not necessary for a dynamical phase transition to have different power laws for $\omega < \omega_c$ and $\omega > \omega_c$. We have seen above that the power law $(1/n^{1/2})$ is the same on the two sides of ω_c for a general initial state, but there is a different power law $(1/n^{1/3})$ exactly at ω_c. However, for a special choice of initial state ($\phi = 0$), the power law is different on the two sides, being $1/n^{1/2}$ for $\omega < \omega_c$ and $1/n^{3/2}$ for $\omega > \omega_c$.

IV. ISING MODEL

For the one-dimensional $S = 1/2$ Ising model with L spins and periodic boundary conditions, the Hamiltonian reads

$$H = -\frac{1}{2}\sum_{j=1}^{L}\left(g\tau_j^x + \tau_j^z\tau_{j+1}^z\right), \tag{65}$$

where $\tau_j^{x,y,z}$ denote the Pauli matrices for the physical spins on site j, we have set the Ising nearest-neighbor interaction to $J = 1/2$, and $g = h/J$ is the dimensionless magnetic field. Carrying out a Jordan-Wigner transformation from spins to spinless fermions with

$$\tau_i^x = 1 - 2c_i^\dagger c_i, \quad \tau_i^z = -\left[\prod_{j<i}(1 - 2c_j^\dagger c_j)\right](c_i^\dagger + c_i), \tag{66}$$

where $c_i^\dagger(c_i)$ creates (destroys) a spinless fermion on site i allows one to rewrite H in Eq. (65) as

$$H = g\sum_{j=1}^{L} c_j^\dagger c_j - \sum_{j=1}^{L-1}(c_j^\dagger c_{j+1} + c_j^\dagger c_{j+1}^\dagger + \text{H.c.})/2 + (-1)^{N_F}(c_L^\dagger c_1 + c_L^\dagger c_1^\dagger + \text{H.c.})/2, \tag{67}$$

where N_F denotes the number of fermions. For the rest, we restrict to even N_F, which implies that $c_{L+1} = -c_1$. Further using

$$c_k = \frac{\exp(i\pi/4)}{\sqrt{L}}\sum_j \exp(-ikj)c_j, \tag{68}$$

where $k = 2\pi m/L$ with $m = -(L-1)/2, \cdots, -1/2, 1/2, \cdots, (L-1)/2$, Eq. (67) can be written as $H = \sum_{k>0} H_k$ where

$$H_k = (g - \cos k)[c_k^\dagger c_k - c_{-k}c_{-k}^\dagger] + \sin k[c_{-k}c_k + c_k^\dagger c_{-k}^\dagger]. \tag{69}$$

This can be recast in the form of Eqs. (2) by noting that since the fermions can be created or destroyed only in pairs, one can introduce pseudospins $|\uparrow\rangle_k = c_k^\dagger c_{-k}^\dagger|0\rangle$ and $|\downarrow\rangle_k = |0\rangle$, where $|0\rangle$ represents the fermion vacuum which gives

$$h_z(k,t) = g(t) - \cos k, \quad h_x(k,t) = \sin k, \quad h_y(k,t) = 0. \tag{70}$$

We concentrate on a square pulse protocol with $g(t) = g_i$ for $0 \leqslant t < T/2$ and $g(t) = g_f$ for $T/2 \leqslant t < T$ following Ref. [46]. Further, without any loss of generality, we choose the initial state to be $(0, 1)^T$ for all k which represents the fermion vacuum or $\tau_i^x = +1$ in terms of the physical spins to study relaxation of local quantities to their final steady state values as a function of n, the number of drive cycles. Equations (71)–(74) follow from the discussion in Ref. [46] and we reproduce these below for ease of presentation. For the choice of initial state and for $L \to \infty$, $\delta C_{ij}(n) = \langle c_i^\dagger c_j\rangle_n - \langle c_i^\dagger c_j\rangle_\infty$ and $\delta F_{ij}(n) = \langle c_i^\dagger c_j^\dagger\rangle_n - \langle c_i^\dagger c_j^\dagger\rangle_\infty$ equal [46]

$$\delta C_{ij}(n) = \int_0^\pi \frac{dk}{2\pi} f_1(k)\cos(2n\phi(k)),$$
$$\delta F_{ij}(n) = \int_0^\pi \frac{dk}{2\pi}\left[f_2(k)\cos(2n\phi(k)) + f_3(k)\sin(2n\phi(k))\right], \tag{71}$$

with

$$f_1(k) = -\left(1 - \hat{n}_z^2(k)\right)\cos(k(i-j)),$$
$$f_2(k) = -i\hat{n}_z(k)f_3(k),$$
$$f_3(k) = i(n_x(k) + in_y(k))\sin(k(i-j)). \tag{72}$$

In Eqs. (72), we used the fact that the Floquet unitary at each k mode can be written as a 2×2 matrix of the form $U_k = \exp[-i\phi(k)\vec{\sigma}\cdot\hat{n}(k)]$ where $\hat{n}(k) = (n_x(k), n_y(k), n_z(k))$ represents a unit vector and $\phi(k) \in [0, \pi]$ in the reduced zone scheme. The Floquet Hamiltonian can be expressed as

$$H_F(k) = \vec{\sigma}\cdot\epsilon(\vec{k}) = \Delta(k)\vec{\sigma}\cdot\hat{n}(k)/2, \tag{73}$$

where $\vec{\epsilon}(k) = (\epsilon_x(k), \epsilon_y(k), \epsilon_z(k))$, $\Delta(k) = 2|\vec{\epsilon}(k)|$ is the Floquet energy gap, and $\hat{n}(k) = \vec{\epsilon}(k)/|\vec{\epsilon}(k)|$. This fixes $\phi(k) = T\Delta(k)/2$ where each component of $\vec{\epsilon}(k)$ is restricted to $[-\pi/T, \pi/T]$ in the reduced zone scheme. The expression of $\vec{\epsilon}(k)$ has been computed in Ref. [46]. For the square pulse

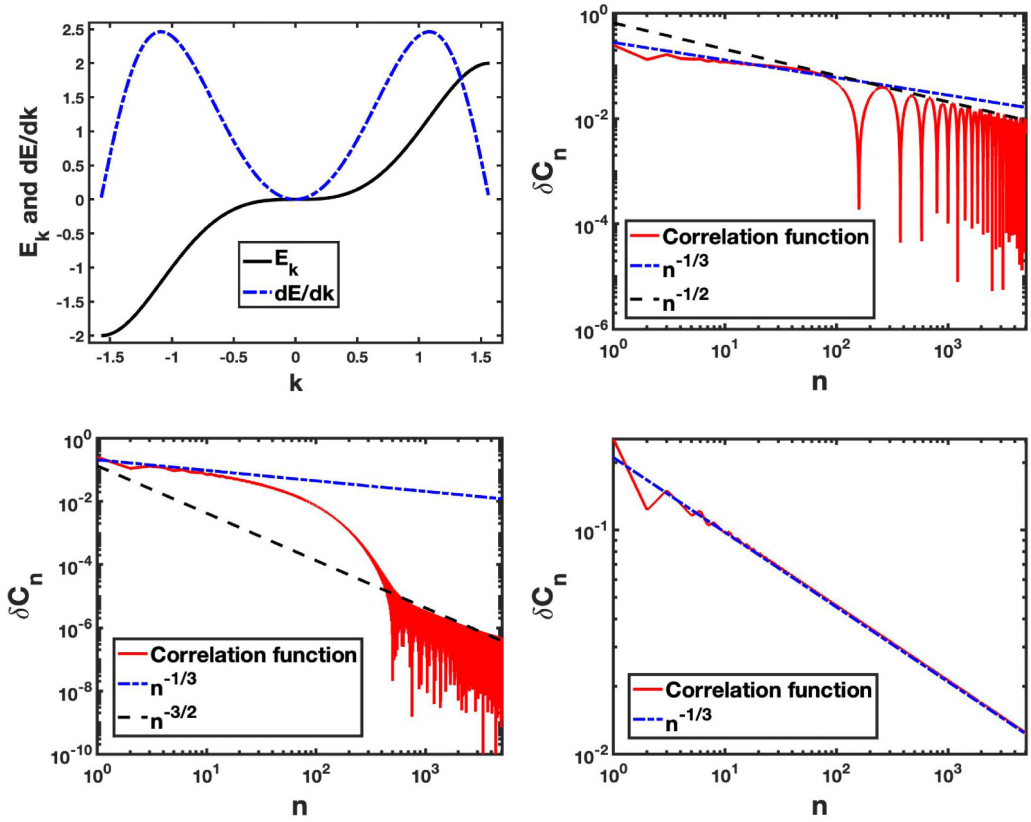

FIG. 5. Top left panel: Plot of the exact numerical Floquet energy (black solid line) and its derivative (blue dot-dashed line) as a function of k, for $\gamma_1 = 1$, $\gamma_2 = -1$, $a = 6$, and $\omega = \omega_c$, where $\omega_c = 4a/\mu_1$. Top right panel: Log-log plot of δC_n computed from exact numerics (for $\phi = 0$ for the initial state) showing $n^{-1/3}$ to $n^{-1/2}$ crossover at $\omega = 4a/(\mu_1 + 0.1)$. Bottom left panel: Same as top right panel but for $\omega = 4a/(\mu_1 - 0.1)$ showing crossover from $n^{-1/3}$ to $n^{-3/2}$ behavior. Bottom right panel: Same as top right panel but for $\omega = \omega_c$ showing $n^{-1/3}$ decay.

protocol which we focus on in this paper, we find

$$\begin{aligned}\Delta(k) &= 2\arccos(M_k/T),\\ M_k &= \cos\Phi_i(k)\cos\Phi_f(k)\\ &\quad -\hat{N}_i(k)\cdot\hat{N}_f(k)\sin\Phi_i(k)\sin\Phi_f(k),\\ \Phi_{i(f)}(k) &= (T/2)\sqrt{(g_{i(f)}-\cos k)^2+\sin^2 k},\\ N_{i(f)}(k) &= (\sin k, 0, (g_{i(f)}-\cos k))T/(2\Phi_{i(f)}(k)).\end{aligned} \quad (74)$$

The square pulse protocol allows for analytic expressions for U_k. From Eqs. (71), the stationary points $d\Delta(k)/dk = 0$ in $k \in [0, \pi]$ determine the behavior of the relaxation of local quantities. As shown in Ref. [46], the number of stationary points in $k \in (0, \pi)$ is 0 for $\omega = 2\pi/T \to \infty$ while it scales as $1/\omega$ as $\omega \to 0$. Importantly, $f_{1,2,3}(k)$ in Eqs. (72) vanish at $k = 0$ and $k = \pi$ for any (g_i, g_f, T) while these are generally nonzero when $k \neq 0, \pi$. Lastly, keeping g_i, g_f, T fixed, a series expansion of $\Delta(k)$ around $k = 0$ and $k = \pi$, respectively, yields only even powers.

For the rest of this section, we focus on $\delta C_{ii}(n)$, which also equals $(1 - \langle\tau_i^x\rangle)/2$ from Eqs. (66) (since the initial state and the drive protocol are both translationally invariant, the dependence on site index i can be dropped) with the other local fermionic correlators also showing similar decays in time. Let us quickly recapitulate the relaxation behavior in the two dynamical phases that are distinguished by whether the stationary points occur only at $k = 0, \pi$ versus the appearance of extra stationary points in $k \in (0, \pi)$. We denote the number of stationary points in $k \in (0, \pi)$ by N_b. First, $\alpha = 2$ ($\alpha = 0$) for stationary points with $k = 0$ or π ($k \neq 0, \pi$) from the behavior of $f_1(k)$. Second, $\beta = 2$ in both cases. This immediately gives a relaxation of $n^{-3/2}$ ($n^{-1/2}$) when $N_b = 0$ ($N_b \neq 0$) from Eq. (1).

We now focus on the relaxation behavior exactly at the dynamical critical points. As discussed in Ref. [46], these come in two varieties—critical points where N_b changes by 1 (e.g., from $N_b = 0$ to $N_b = 1$) and critical points where N_b changes by two (e.g., from $N_b = 2$ to $N_b = 0$). The former class arises due to an extra stationary point entering from either $k = 0$ or π [where $f_i(k) = 0$ for $i = 1, 2, 3$] [46], and the latter class arises due to two stationary points in $k \in (0, \pi)$, coalescing to one at the critical point [Fig. 6 (top left)] as the drive frequency is tuned, keeping g_i, g_f fixed. The first dynamical transition as ω is reduced from very large values always belongs to the first category, while some other dynamical transitions may belong to the second category as ω is lowered further. For the first category, $\alpha = 2$ since the extra stationary point emerges from either $k = 0$ or π. Here $\beta = 4$ since although the critical point requires that $d^2\Delta(k)/dk^2 = 0$ at $k = 0$ or π, we also have $d^3\Delta(k)/dk^3 = 0$ at these two momenta. These two facts imply a critical relaxation of $n^{-3/4}$ from Eq. (1). For the

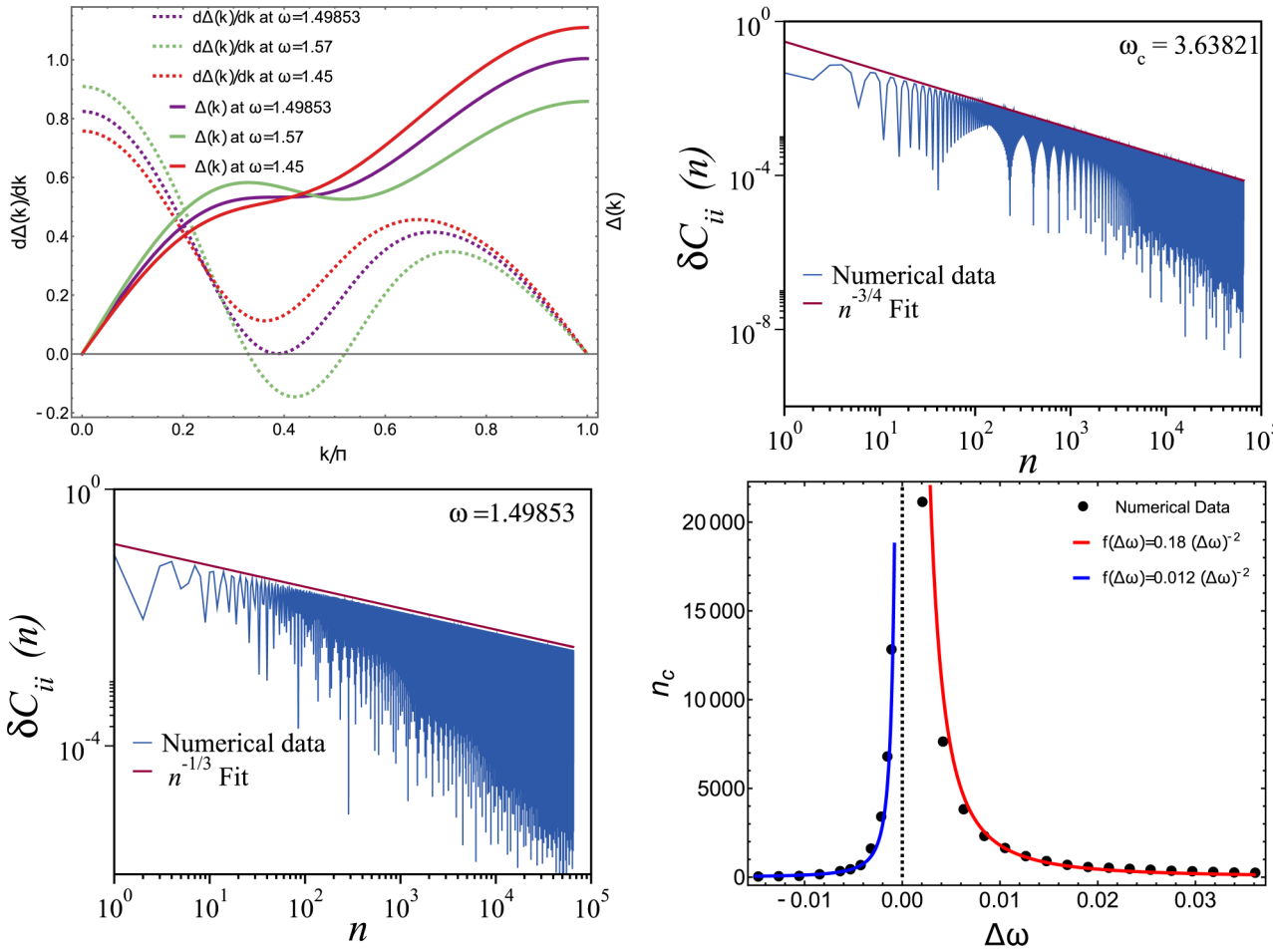

FIG. 6. Top left panel: $\Delta(k)$ (solid lines) and $d\Delta(k)/dk$ (dotted lines) as a function of k for various values of ω. The dynamical critical point of the second type is characterized by $N_b = 1$ with this stationary point also being a minimum of $d\Delta(k)/dk$ as the drive frequency is tuned. Top right and bottom left panels: Relaxation of a local quantity $\delta C_{ii}(n)$ shown as a function of n for a dynamical critical point of the first type and second type (bottom left), respectively. Bottom right panel: The behavior of the crossover timescale, n_c, as the drive frequency ω is tuned to $\omega_c \approx 3.63821$ from both sides.

second category, the single stationary point in $k \in (0, \pi)$ also becomes a minimum of $d\Delta(k)/dk$ [Fig. 6 (top left)]. Thus, $\alpha = 0$ and $\beta = 3$ for this point since $k \neq 0, \pi$ and $f_1(k) \neq 0$ generically for $k \in (0, \pi)$. This gives a critical relaxation of $n^{-1/3}$ from Eq. (1) for these critical points.

We now show results for $g_i = 2$ and $g_f = 0$, where both types of dynamical critical points can be accessed by tuning the drive frequency ω by using a system size of $L = 8 \times 10^5$ to minimize finite-size effects. For $\omega \approx 3.63821$, we encounter the first dynamical critical transition where N_b changes from 0 to 1 across the transition while for $\omega \approx 1.49853$, we encounter a dynamical transition where N_b changes from 2 to 0. Fig. 6 (top right) shows the relaxation to be $n^{-3/4}$ for the former case and Fig. 6 (bottom left) shows the relaxation to be $n^{-1/3}$ for the latter case, completely in accord with our theoretical expectation. Furthermore, we expect a diverging dynamical crossover timescale n_c in the vicinity of the critical points in both the dynamical phases where the relaxation of local quantities scale as $n^{-3/4}$ ($n^{-1/3}$) for $n \ll n_c$ before crossing over to $n^{-3/2}$ or $n^{-1/2}$ for $n \gg n_c$. We extract n_c from our numerical data and show its behavior in the vicinity of the first dynamical phase transition in Fig. 6 (bottom right). Expectedly, n_c shows a divergence as the critical point is approached from both sides. The crossover scale n_c is determined by fitting the early (late) time data for $\delta C_{ii}(n)$ to $n^{-3/4}$ ($n^{-3/2}$ or $n^{-1/2}$) and extracting the crossing point of the fitted lines in a log-log plot [see Fig. 7 (left and right panels)].

We now discuss how n_c diverges near the first dynamical phase transition as ω approaches ω_c from above. Referring to Eq. (17), we see that here $\beta_0 = 4$ and $a_0 = 2$ since the extra stationary point enters from $k = \pi$ for the square pulse protocol [46] where only even powers contribute. Thus, $n_c \sim (c_2/c_1)^2$ and the divergence occurs since $c_1 = 0$ exactly at the critical point. Furthermore, c_1 changes sign as ω is changed from above to below the critical frequency, which implies that $c_1 \sim \omega - \omega_c$ near the transition. This fixes $n_c \sim (\omega - \omega_c)^{-2}$ as one approaches the dynamical critical point from above. In contrast, for approaching the point from below, we need to take into account the fact that there are two stationary points (at $k = \pi$ and $\pi - k_0$ where $k_0 \sim \sqrt{\omega_c - \omega}$) which approach each other as one nears the critical point. Numerically, c_1 is small and $|c_1|$ is of the same order for both stationary points. The characteristic around this stationary point controls n_c and numerically we find that the same scaling (as the one

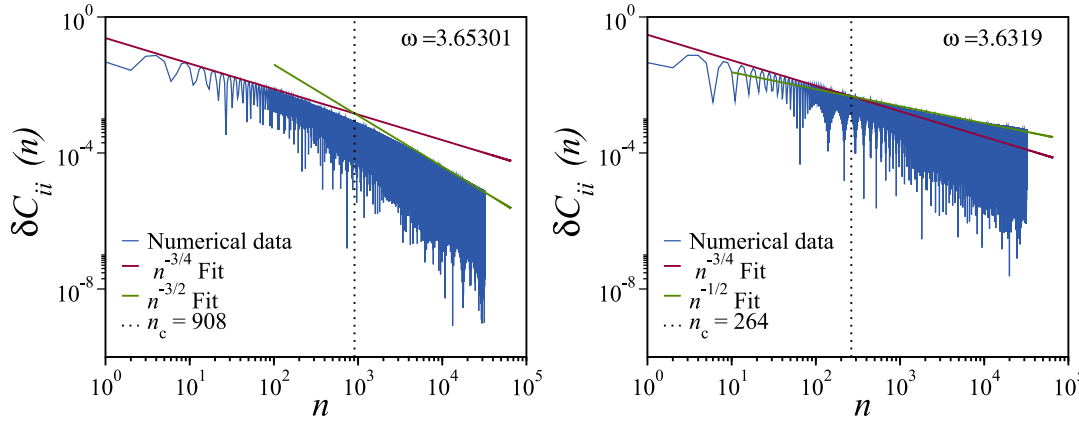

FIG. 7. The behavior of $\delta C_{ii}(n)$ for $\omega > \omega_c$ (left panel) and $\omega < \omega_c$ (right panel) in the vicinity of the first dynamical critical point ($\omega_c \approx 3.63821$) with $g_i = 2$, $g_f = 0$ shows the presence of a dynamical crossover from critical scaling ($n^{-3/4}$) to noncritical scaling ($n^{-3/2}$ in the left panel and $n^{-1/2}$ in the right panel).

when the critical point is approached from above) holds in this case. This is shown in the right panel of Fig. 7. A plot of the correlation function for two representative values of $\omega < \omega_c$ is shown in the left panel of Fig. 8. The plot reveals a long-time oscillation of the correlation function, similar to that identified for the SSH model in the previous section, with $\Delta n = 1400(260)$ for $\omega = 3.6361(3.63505)$. The time period Δn of these oscillations diverges as ω approaches ω_c in accordance with that found for the SSH model in Sec. III. An analysis along the same line as in the SSH model predicts $1/k_0^4$ divergence, where $k_0 \sim \sqrt{|\omega - \omega_c|}$ is the distance between the extrema (at $k = \pi$ and $k = \pi - k_0$) in the Floquet Brillouin zone. This fits the data for large k_0; however, it breaks down when k_0 is small where a much faster divergence is encountered; this is probably due to the proximity of the two symmetry-unrelated stationary points in the Brillouin zone as well as the small value of $d\Delta(k)/dk$ near them. These features probably invalidate an analysis based on the premise that the contribution to the correlation function comes only from the two stationary points.

V. DISCUSSION

In this paper, we have studied the dynamical relaxation of correlation functions to their steady-state values in driven 1D integrable quantum models as a function of the number of drive cycles n. We summarize the generic behavior of such relaxation by identifying a general power law in terms of two positive integers α and β. The exponents corresponding to $\beta = 2$ and different α characterizes different dynamical phases; this was identified in Ref. [46]. Here we find the presence of other possible exponents characterized by $\beta = 3$ and $\beta = 4$. These anomalous exponents typically occur at the dynamical transition between two dynamical phases; however, they may also occur at special points within a dynamical phase. We provide a general analysis of the behavior of such correlation functions in terms of the Floquet spectrum of the driven model and show that their occurrence is tied to points of inflections in the Floquet spectrum. At these points, for a Floquet spectrum which is odd under $k \to -k$, the correlation functions decay with $\beta = 3$; for an even spectrum, we find a decay with $\beta = 4$.

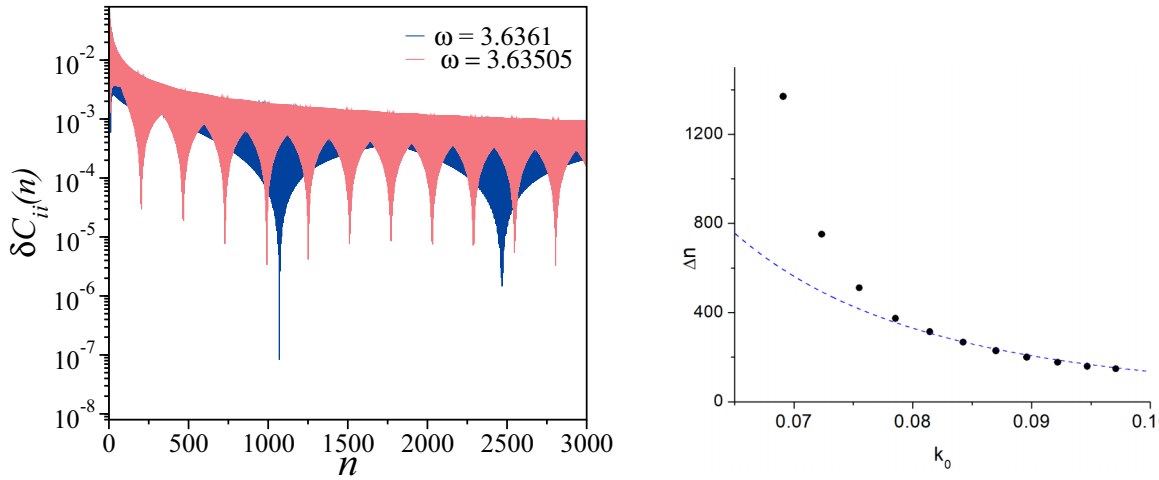

FIG. 8. Left panel: The behavior of $\delta C_{ii}(n)$ for two representative values of $\omega < \omega_c \simeq 3.638$ showing long-time coherent oscillations corresponding to $\Delta n \simeq 1400$ ($\omega = 3.6361$) and $\Delta n \simeq 260$ ($\omega = 3.63505$). For both plots $g_i = 2$ and $g_f = 0$, and ω_c corresponds to the first transition frequency. Right panel: A plot of the oscillation period Δn to the distance k_0 between the two extrema of H_F (at $k = \pi$ and $k = \pi - k_0$) in the Floquet Brillouin zone showing $1/k_0^4$ (the dashed blue line corresponds to $0.0135/k_0^4$) behavior at larger k_0.

This analysis also points to the absence of such anomalous powers ($\beta \neq 2$) for dynamical transitions in higher dimensional integrable models. The presence of the anomalous exponent requires the existence of a point of inflection in the Floquet spectrum; for $d > 1$, this requires vanishing of multiple derivatives $\partial^2\Delta/\partial k_i \partial k_j$ at such a point. Since the transition can be reached by tuning a single parameter, namely, the drive frequency, multiple derivatives cannot generically vanish at the transition. Thus we expect such anomalous exponents to be realized only for 1D models.

We have studied two concrete models to show the existence of such anomalous decay. The first one involves the SSH model driven by a continuous protocol; this model realizes decay of correlations with $\beta = 3$ leading to a $n^{-1/3}$ behavior. We analyze the driven SSH model within first-order FPT to gain analytical insight into the problem; the results of the first-order FPT agrees almost identically with the exact numerical study. We also study the correlation functions of the 1D transverse field Ising model. The model shows a reentrant transition between two dynamical phases at several drive frequencies. We show that the correlation function decays with $\beta = 4$ at the first (highest frequency) transition, leading to a $n^{-3/4}$ behavior. In contrast, the subsequent transitions at lower drive frequency exhibit $n^{-1/3}$ decay and correspond to $\beta = 3$.

Near these transitions which host relaxation with anomalous power laws, we find a crossover scale, n_c, after which the correlators decay to their steady-state values with exponents corresponding to $\beta = 2$. Such crossover scales can be identified at both sides of the transition. It was found that $n_c \sim (\omega - \omega_c)^{-\beta_0/(\beta_0 - a_0)}$; thus it exhibits a power-law divergence at the transition. This behavior has been confirmed from exact numerics for both the Ising and the SSH model. The former model exhibits $\beta_0 = 4$ and $a_0 = 2$, leading to $n_c \sim (\omega - \omega_c)^{-2}$ at the first dynamical transition, while the second model corresponds to $\beta_0 = 3$ and $a_0 = 1$ leading to $n_c \sim |\omega - \omega_c|^{-3/2}$.

Finally, our analysis shows a long-time oscillatory behavior of the correlation functions near the transition at ω_c. Such behavior is seen when the transition is approached from below ω_c and is seen in both models. Our FPT analysis for the SSH model shows that such an oscillation results from the presence of two stationary points (at $k = \pm k_0$) and provides an analytical estimate of the time period of such oscillations. This estimate shows a near-exact match with results from exact numerics. However, for the Ising model, a similar analysis fails to capture the time period when the two stationary points are close to each other (small k_0); this failure could be due to proximity of symmetry-unrelated stationary points and the flat nature of $\Delta(k)$ around $k = \pi$ near the transition. This leads to near-zero values of $d\Delta(k)/dk$ for several values of k between the two stationary points (at $k = \pi$ and $\pi - k_0$); as a result, the correlators receive contributions from all these momenta. This may invalidate an analysis based on contributions from only the two stationary points; we leave a further study of this issue for future work.

In conclusion, we have studied the dynamical relaxation of correlation function of driven 1D quantum integrable models. We have identified anomalous power laws characterizing the decay of these correlators to their steady-state value as a function of the number of drive cycles and a diverging crossover timescale as the dynamical transition is approached from both sides. Our analysis also reveals a long-time oscillatory behavior of these correlation functions near a dynamical transition when the transition is approached from the low-frequency side.

Note added: Recently, we came to know about a similar work unraveling anomalous power laws by Makki *et al.* [60]. Our results agree wherever a comparison is possible.

ACKNOWLEDGMENTS

S.A. thanks MHRD, India for financial support through a PMRF. D.S. thanks SERB, India for funding through Project No. JBR/2020/000043. We thank Amit Dutta for discussions of their work on anomalous power laws.

[1] J. Dziarmaga, Adv. Phys. **59**, 1063 (2010).
[2] A. Polkovnikov, K. Sengupta, A. Silva, and M. Vengalattore, Rev. Mod. Phys. **83**, 863 (2011).
[3] A. Dutta, G. Aeppli, B. K. Chakrabarti, U. Divakaran, T. F. Rosenbaum, and D. Sen, *Quantum Phase Transitions in Transverse Field Spin Models: From Statistical Physics to Quantum Information* (Cambridge University Press, Cambridge, 2015).
[4] S. Mondal, D. Sen, and K. Sengupta, in *Quantum Quenching, Annealing and Computation*, edited by A. K. Chandra, A. Das, and B. K. Chakrabarti, Lecture Notes in Physics Vol. 802 (Springer, Berlin, Heidelberg, 2010), Chap. 2, pp. 21–56; C. De Grandi and A. Polkovnikov, *ibid*, Chap 6, pp. 75–114.
[5] M. Bukov, L. D'Alessio, and A. Polkovnikov, Adv. Phys. **64**, 139 (2015); L. D'Alessio and A. Polkovnikov, Ann. Phys. **333**, 19 (2013).
[6] L. D'Alessio, Y. Kafri, A. Polkovnikov, and M. Rigol, Adv. Phys. **65**, 239 (2016).
[7] A. Sen, D. Sen, and K. Sengupta, J. Phys.: Condens. Matter **33**, 443003 (2021).
[8] K. Sengupta, S. Powell, and S. Sachdev, Phys. Rev. A **69**, 053616 (2004).
[9] P. Calabrese and J. Cardy, Phys. Rev. Lett. **96** 136801 (2006); J. Stat. Mech.: Theory Exp. (2007) P06008.
[10] C. De Grandi, V. Gritsev, and A. Polkovnikov, Phys. Rev. B **81**, 012303 (2010).
[11] A. Polkovnikov, Phys. Rev. B **72**, 161201(R) (2005); A. Polkovnikov and V. Gritsev, Nat. Phys. **4**, 477 (2008).
[12] B. Damski, Phys. Rev. Lett. **95**, 035701 (2005); J. Dziarmaga, *ibid.* **95**, 245701 (2005); J. Dziarmaga, J. Meisner, and W. H. Zurek, *ibid.* **101**, 115701 (2008); R. W. Cherng and L. S. Levitov, Phys. Rev. A **73**, 043614 (2006).
[13] D. Sen, K. Sengupta, and S. Mondal, Phys. Rev. Lett. **101**, 016806 (2008); S. Mondal, K. Sengupta, and D. Sen, Phys. Rev. B **79**, 045128 (2009).

[14] K. Sengupta, D. Sen, and S. Mondal, Phys. Rev. Lett. **100**, 077204 (2008); S. Mondal, D. Sen, and K. Sengupta, Phys. Rev. B **78**, 045101 (2008).

[15] U. Divakaran, A. Dutta, and D. Sen, Phys. Rev. B **78**, 144301 (2008); V. Mukherjee, A. Dutta, and D. Sen, *ibid.* **77**, 214427 (2008); U. Divakaran, V. Mukherjee, A. Dutta, and D. Sen, J. Stat. Mech.: Theory Exp. (2009) P02007.

[16] C. Trefzger and K. Sengupta, Phys. Rev. Lett. **106**, 095702 (2011).

[17] S. Nandy, A. Sen, and D. Sen, Phys. Rev. X **7**, 031034 (2017); Phys. Rev. B **98**, 245144 (2018).

[18] A. Verdeny, J. Puig, and F. Mintert, Z. Naturforsch. A **71**, 897 (2016); P. T. Dumitrescu, R. Vasseur, and A. C. Potter, Phys. Rev. Lett. **120**, 070602 (2018).

[19] S. Ray, S. Sinha, and D. Sen, Phys. Rev. E **100**, 052129 (2019); D. V. Else, W. W. Ho, and P. T. Dumitrescu, Phys. Rev. X **10**, 021032 (2020).

[20] H. Zhao, F. Mintert, R. Moessner, and J. Knolle, Phys. Rev. Lett. **126**, 040601 (2021).

[21] B. Mukherjee, A. Sen, D. Sen, and K. Sengupta, Phys. Rev. B **102**, 014301 (2020).

[22] I. Bloch, J. Dalibard, and W. Zwerger, Rev. Mod. Phys. **80**, 885 (2008); L. Taurell and L. Sanchez-Palencia, C. R. Phys. **19**, 365 (2018).

[23] M. Greiner, O. Mandel, T. Esslinger, T. W. Hänsch, and I. Bloch, Nature (London) **415**, 39 (2002); C. Orzel, A. K. Tuchman, M. L. Fenselau, M. Yasuda, and M. A. Kasevich, Science **291**, 2386 (2001).

[24] T. Kinoshita, T. Wenger, and D. S. Weiss, Nature (London) **440**, 900 (2006); L. E. Sadler, J. M. Higbie, S. R. Leslie, M. Vengalattore, and D. M. Stamper-Kurn, *ibid.* **443**, 312 (2006).

[25] W. S. Bakr, J. Gillen, A. Peng, S. Fölling, and M. Greiner, Nature (London) **462**, 74 (2009).

[26] W. S. Bakr, A. Peng, M. E. Tai, R. Ma, J. Simon, J. I. Gillen, S. Fölling, L. Pollet, and M. Greiner, Science **329**, 547 (2010).

[27] H. Bernien, S. Schwartz, A. Keesling, H. Levine, A. Omran, H. Pichler, S. Choi, A. S. Zibrov, M. Endres, M. Greiner, V. Vuletic, and M. D. Lukin, Nature (London) **551**, 579 (2017); H. Levine, A. Keesling, A. Omran, H. Bernien, S. Schwartz, A. S. Zibrov, M. Endres, M. Greiner, V. Vuletic, and M. D. Lukin, Phys. Rev. Lett. **121**, 123603 (2018).

[28] T. Kitagawa, E. Berg, M. Rudner, and E. Demler, Phys. Rev. B **82**, 235114 (2010); N. H. Lindner, G. Refael, and V. Galitski, Nat. Phys. **7**, 490 (2011); T. Kitagawa, T. Oka, A. Brataas, L. Fu, and E. Demler, Phys. Rev. B **84**, 235108 (2011).

[29] M. Thakurathi, A. A. Patel, D. Sen, and A. Dutta, Phys. Rev. B **88**, 155133 (2013); A. Kundu, H. A. Fertig, and B. Seradjeh, Phys. Rev. Lett. **113**, 236803 (2014).

[30] F. Nathan and M. S. Rudner, New J. Phys. **17**, 125014 (2015); B. Mukherjee, A. Sen, D. Sen, and K. Sengupta, Phys. Rev. B **94**, 155122 (2016); B. Mukherjee, P. Mohan, D. Sen, and K. Sengupta, *ibid.* **97**, 205415 (2018).

[31] V. Khemani, A. Lazarides, R. Moessner, and S. L. Sondhi, Phys. Rev. Lett. **116**, 250401 (2016).

[32] D. V. Else, B. Bauer, and C. Nayak, Phys. Rev. Lett. **117**, 090402 (2016).

[33] J. Zhang, P. W. Hess, A. Kyprianidis, P. Becker, A. Lee, J. Smith, G. Pagano, I.-D. Potirniche, A. C. Potter, A. Vishwanath, N. Y. Yao, and C. Monroe, Nature (London) **543**, 217 (2017).

[34] T. Nag, S. Roy, A. Dutta, and D. Sen, Phys. Rev. B **89**, 165425 (2014); T. Nag, D. Sen, and A. Dutta, Phys. Rev. A **91**, 063607 (2015).

[35] A. Agarwala, U. Bhattacharya, A. Dutta, and D. Sen, Phys. Rev. B **93**, 174301 (2016); A. Agarwala and D. Sen, *ibid.* **95**, 014305 (2017).

[36] D. J. Luitz, Y. Bar Lev, and A. Lazarides, SciPost Phys. **3**, 029 (2017); D. J. Luitz, A. Lazarides, and Y. Bar Lev, Phys. Rev. B **97**, 020303(R) (2018).

[37] R. Ghosh, B. Mukherjee, and K. Sengupta, Phys. Rev. B **102**, 235114 (2020).

[38] A. Das, Phys. Rev. B **82**, 172402 (2010); S. Bhattacharyya, A. Das, and S. Dasgupta, *ibid.* **86**, 054410 (2012); S. S. Hegde, H. Katiyar, T. S. Mahesh, and A. Das, *ibid.* **90**, 174407 (2014).

[39] S. Mondal, D. Pekker, and K. Sengupta, Europhys. Lett. **100**, 60007 (2012); U. Divakaran and K. Sengupta, Phys. Rev. B **90**, 184303 (2014).

[40] S. Iubini, L. Chirondojan, G.-L. Oppo, A. Politi, and P. Politi, Phys. Rev. Lett. **122**, 084102 (2019).

[41] B. Mukherjee, S. Nandy, A. Sen, D. Sen, and K. Sengupta, Phys. Rev. B **101**, 245107 (2020).

[42] B. Mukherjee, A. Sen, D. Sen, and K. Sengupta, Phys. Rev. B **102**, 075123 (2020).

[43] M. Heyl, A. Polkovnikov, and S. Kehrein, Phys. Rev. Lett. **110**, 135704 (2013); M. Heyl, Rep. Prog. Phys. **81**, 054001 (2018); Phys. Rev. Lett. **115**, 140602 (2015).

[44] C. Karrasch and D. Schuricht, Phys. Rev. B **87**, 195104 (2013); J. N. Kriel and C. Karrasch, and S. Kehrein, *ibid.* **90**, 125106 (2014); F. Andraschko and J. Sirker, *ibid.* **89**, 125120 (2014); E. Canovi, P. Werner, and M. Eckstein, Phys. Rev. Lett. **113**, 265702 (2014).

[45] S. Sharma, U. Divakaran, A. Polkovnikov, and A. Dutta, Phys. Rev. B **93**, 144306 (2016); S. Bandyopadhyay, A. Polkovnikov, and A. Dutta, Phys. Rev. Lett. **126**, 200602 (2021).

[46] A. Sen, S. Nandy, and K. Sengupta, Phys. Rev. B **94**, 214301 (2016).

[47] S. Nandy, K. Sengupta, and A. Sen, J. Phys. A **51**, 334002 (2018).

[48] M. Sarkar and K. Sengupta, Phys. Rev. B **102**, 235154 (2020).

[49] S. E. Tapias Arze, P. W. Clayes, I. P. Castillo, and J.-S. Caux, SciPost Phys. Core **3**, 001 (2020).

[50] S. Sachdev, *Quantum Phase Transitions* (Cambridge University Press, Cambridge, England, 1999).

[51] W. P. Su, J. R. Schrieffer, and A. J. Heeger, Phys. Rev. Lett. **42**, 1698 (1979).

[52] A. Soori and D. Sen, Phys. Rev. B **82**, 115432 (2010).

[53] T. Bilitewski and N. R. Cooper, Phys. Rev. A **91**, 063611 (2015).

[54] J. K. Asbóth, B. Tarasinski, and P. Delplace, Phys. Rev. B **90**, 125143 (2014).

[55] W. Zheng and H. Zhai, Phys. Rev. A **89**, 061603(R) (2014).

[56] O. Balabanov and H. Johannesson, Phys. Rev. B **96**, 035149 (2017).

[57] O. Balabanov and H. Johannesson, J. Phys.: Condens. Matter **32**, 015503 (2020).

[58] D. J. Yates, A. G. Abanov, and A. Mitra, Comm. Phys. **5**, 43 (2022).

[59] C. Borja, E. Gutiérrez, and A. López, arXiv:2111.05500.

[60] A. A. Makki, S. Bandyopadhyay, S. Maity, and A. Dutta, Phys. Rev. B **105**, 054301 (2022).